Supporting Information for:

RNA tertiary structure analysis by 2'-hydroxyl molecular interference

Philip J. Homan[1], Arpit Tandon[2], Greggory M. Rice[1], Feng Ding[3], Nikolay V. Dokholyan[2], Kevin M. Weeks[1,*]

Departments of [1]Chemistry and [2]Biochemistry and Biophysics, University of North Carolina, Chapel Hill, NC 27599-3290, USA
Department of [3]Physics and Astronomy, Clemson University, Clemson, SC 29631, USA

* correspondence, weeks@unc.edu

Supporting Table and Legends

Table S1. DMD simulation statistics for RNA fold refinements. Cluster populations (*n*), mean RMSDs, cluster energies, and *p*-values for each structure are shown.

Figure S1. Electropherograms of 2'-*O*-ester modified and unmodified RNAs. Each RNA was modified with NMIA under denaturing conditions. Modifications were detected as stops to reverse transcriptase-mediated primer extension.

Figure S2. Calculation of RNA HMX scores by normalization and cross-correlation. **(A)** Electropherograms of unfolded RNA (green) scaled to data for folded RNA populations (black). Positions with high intensities in the unfolded RNA have low intensities in the folded RNA. **(B)** Cross-correlation normalization, based on both unfolded and folded 2'-*O*-adduct profiles, was used to create HMX score profiles. Positions with low, medium, and high HMX scores are black, orange, and red, respectively. Experiments were performed in triplicate and error bars are shown with black lines.

Figure S3. Analysis of RNA HMX scores by normalization and cross-correlation for *Tetrahymena* group I intron. HMX profiles were created for each intermediate and the unfolded band. **(A)** Electropherograms of unfolded RNA (green) scaled to data for folded RNA populations (black). **(B)** Cross-correlation normalization, based on both unfolded and folded 2'-*O*-adduct profiles, used to create HMX score histograms. Positions with low, medium, and high HMX scores are black, orange, and red, respectively.

RNA	Cluster	*n*	RMSD (Å)	Energy	*p*-value
M-Box	1	100	13.7 ± 1.3	-79.9 ± 2.0	$<1 \times 10^{-6}$
P546	1	93	19.8 ± 1.2	-78.5 ± 2.2	5.2×10^{-3}
	2	7	24.2 ± 0.4	-70.6 ± 1.1	4.6×10^{-1}
TPP	1	67	8.3 ± 1.0	-38.1 ± 1.7	8.4×10^{-4}
	2	33	11.6 ± 1.0	-38.6 ± 1.4	3.7×10^{-2}
$tRNA^{Asp}$	1	43	18.7 ± 1.3	-35.0 ± 0.9	1.0
	2	13	14.1 ± 1.1	-34.8 ± 0.7	5.2×10^{-1}
	3	12	15.3 ± 0.9	-35.1 ± 0.9	7.5×10^{-1}
	4	9	15.4 ± 0.5	-34.9 ± 0.5	7.7×10^{-1}
	5	8	17.1 ± 1.3	-34.6 ± 0.8	9.6×10^{-1}
	6	6	12.5 ± 1.1	-34.4 ± 0.6	2.0×10^{-1}
	7	5	13.6 ± 0.9	-34.8 ± 0.7	3.9×10^{-1}
	8	2	15.9 ± 0.2	-35.6 ± 0.1	8.4×10^{-1}
	9	1	18.7 ± na	-35.3 ± na	1.0
	10	1	7.6 ± na	-34.8 ± na	1.7×10^{-4}

Homan et al., Table S1

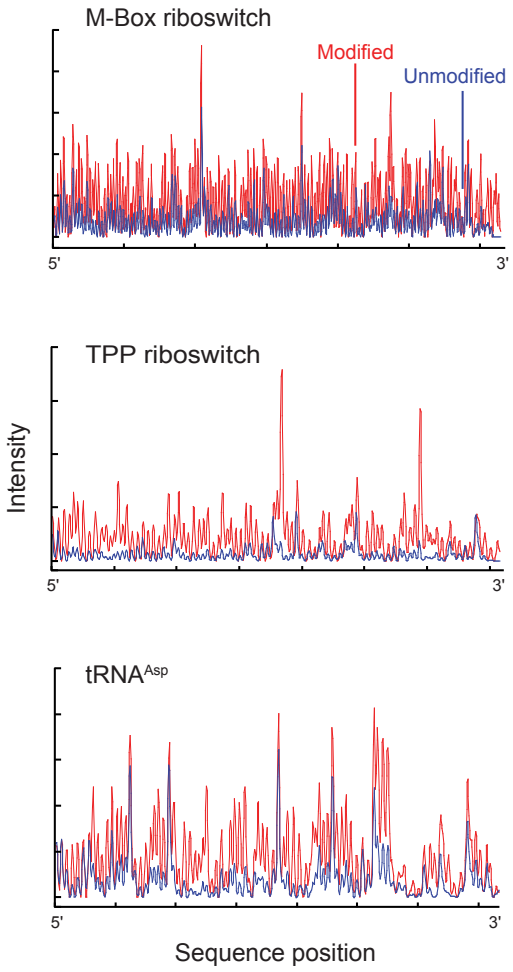

Homan et al., Supporting Fig. 1

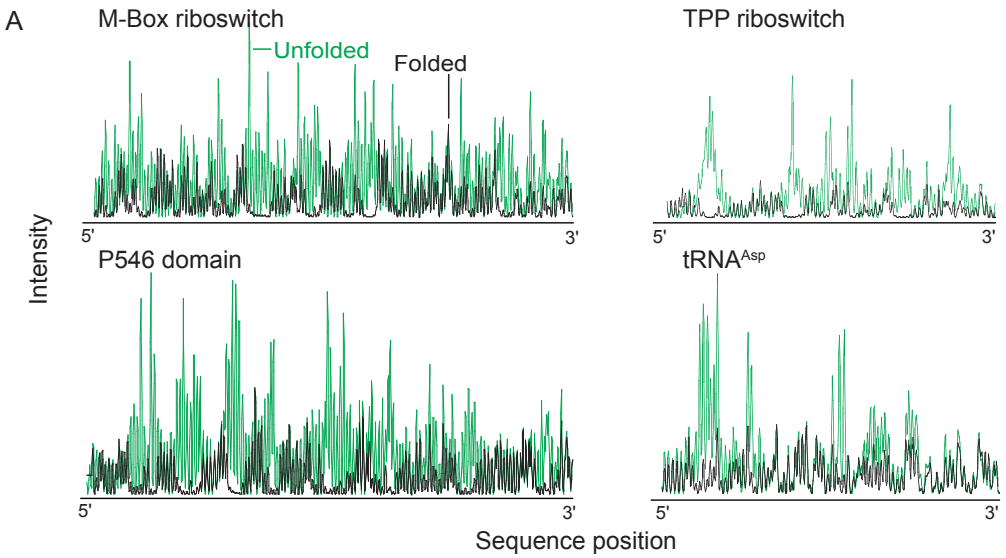

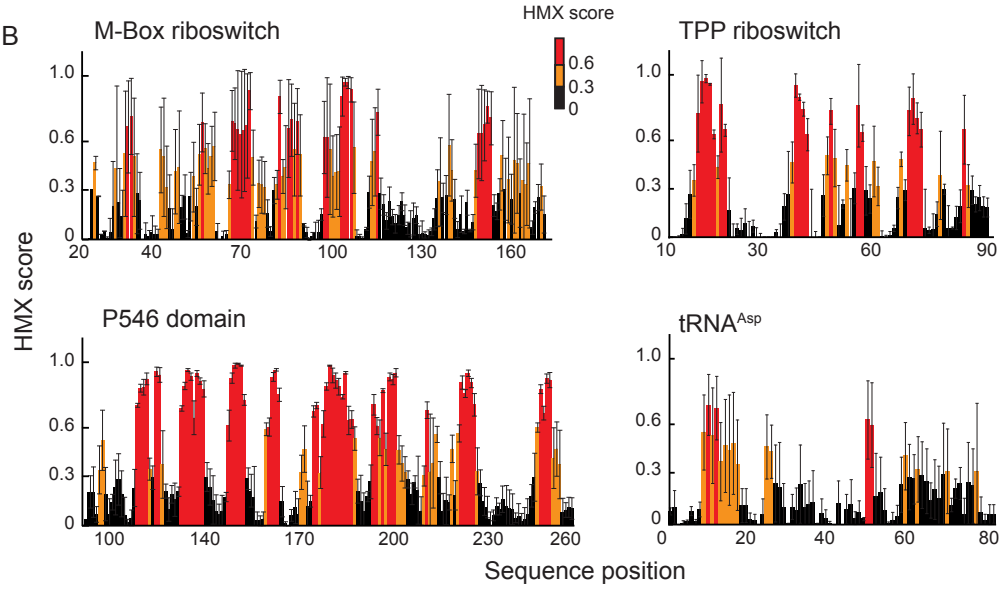

Homan et al., Supporting Fig. 2

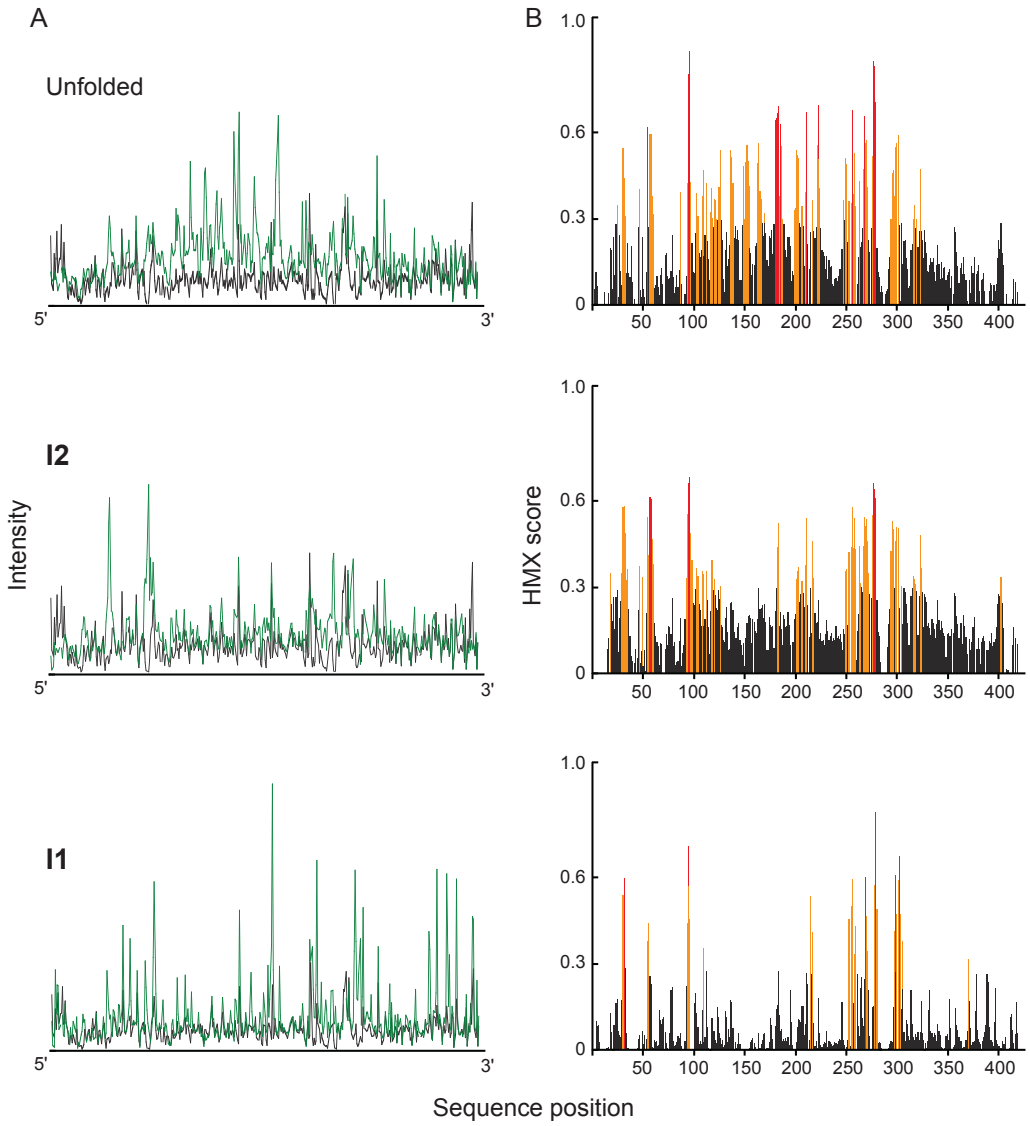

Homan et al., Supporting Fig. 3